

# 用拉曼光谱研究不同吐丝方式获得的蜘蛛牵引丝的二级结构

张磊<sup>1,2</sup>, 鲍先巡<sup>2</sup>, 刘明辉<sup>2</sup>, 韩冷<sup>1</sup>, 中垣雅雄<sup>1</sup>

(1. 信州大学纤维学部应用生物系, 长野 386-8567; 2. 安徽农业科学院蚕桑研究所, 合肥 230061)

**摘要:** 利用傅里叶变换拉曼光谱技术对不同吐丝环境下获得的棒络新妇蜘蛛牵引丝(自由爬行分泌的牵引丝, 垂直下落时分泌的牵引丝, 在 20 mm·s<sup>-1</sup> 的速度下人工强制抽取的牵引丝) 纤维大分子结构进行了分析, 对特征谱带的分析结果表明, 蜘蛛牵引丝蛋白中包含了  $\beta$ -折叠,  $\beta$ -转角,  $\alpha$ -螺旋以及无规卷曲结构; 酰胺 I 带中, 不同的方式获得的牵引丝中所含的 4 种二级结构的比例不同。其中人工强制抽取获得的牵引丝中包含较多的  $\beta$ -折叠结构,  $\alpha$ -螺旋含量最少, 说明在不同环境条件下, 蜘蛛分泌牵引丝的结构会发生变化, 这一改变可能会导致丝纤维的力学特性的改变。

**关键词:** 傅里叶变换拉曼光谱; 牵引丝; 分子结构

中图分类号: TS102.3

文献标识码: A

文章编号: 1672-352X (2013)01-0144-05

## Secondary structure analysis of spider dragline silk fibers obtained by different spinning methods using Raman spectroscopy

ZHANG Lei<sup>1,2</sup>, BAO Xian-xun<sup>2</sup>, LIU Ming-hui<sup>2</sup>, HAN Leng<sup>1</sup>, Nakagaki Masao<sup>1</sup>

(1. Division of Applied Biology, Faculty of Textile Science and Technology, Shinshu University, Nagano 386-8567, Japan;

2. Sericultural Research Institute, Anhui Academy of Agricultural Sciences, Hefei 230061)

**Abstract:** Raman spectra of *Nephia clavata* spider dragline silk fibers were obtained by three different spinning methods: crawl spinning, drop spinning and artificial reeling at 20 mm/s. Based on a rational decomposition of the amide I spectra, the structural conformation of dragline silk proteins and the proportion of those secondary structure were determined. This analysis shows that spider dragline silk contains  $\beta$ -sheet,  $\beta$ -turn,  $\alpha$ -helix and un-ordered structure elements; however, the proportions in which these structures appear changes with the spinning method. The  $\beta$ -sheet content of silk fiber obtained by artificial reeling at 20 mm/s is higher than that of spider spun fibers, indicating that some of the  $\alpha$ -helix and other structures are transformed into  $\beta$ -sheet during the spider's spinning process.

**Key words:** Raman spectroscopy; dragline silk fiber; molecular structure

## 1 Introduction

Silk, one of the most well-known biopolymers, possesses all of the most desirable textile fiber properties: superb fineness, strength, elasticity, dyeability, softness, flexibility, smoothness, luster, and elegance<sup>[1-2]</sup>. Among silk fibers, spider silk has aroused considerable interest due to its combination of unique high tensile strength and extensibility<sup>[3]</sup>. Some spiders can spin seven different types of silk, the strongest of these, dragline silk, is one of the toughest materials

known to man<sup>[4]</sup>. Orb-web spiders use dragline silk from their major ampullate glands as the radial threads in their webs. This silk also allows them to descend very fast<sup>[5]</sup>.

The source of spider silk's remarkable properties has been attributed to the specific secondary and tertiary structures of proteins in the fiber<sup>[6]</sup>. Dragline silk is secreted by the major ampullate gland, which gives rise to a hierarchically organized, semicrystalline material. The crystalline phase is made of short polyaniline segments that adopt a  $\beta$ -sheet conformation.

收稿日期: 2012-11-12

基金项目: 安徽省国际合作项目 (12030603008) 资助。

作者简介: 张磊, 男, 博士。E-mail: micro-stone@hotmail.com

Recent investigations have revealed that  $\beta$ -sheet crystals play a key role in the mechanical properties of silk<sup>[7]</sup>, improving strength and stiffness.

Silk structural properties and mechanical performance depend on spinning condition<sup>[8]</sup>. Variation in both the internal environment (e.g. pH<sup>[9-10]</sup> and temperature<sup>[11]</sup>) of the spider's silk gland and external conditions (e.g. drawing speed<sup>[12]</sup> and humidity<sup>[13]</sup>) under which fibers are pulled from the spinnerets can influence silk properties. In addition, spiders maintain great control over the structure and mechanical properties of silk fibers via changes in the chemical composition of the liquid silk drop<sup>[14]</sup>.

Raman spectra can provide information on the micro-environment and chemistry of a protein polypeptide backbone<sup>[15]</sup>. Alterations in the Raman bands provide information on changes within secondary structures of proteins as well as those in the local environments<sup>[16]</sup>. Raman spectroscopy is also a valuable technique for analyzing mechanical properties of a material because Raman bands shift the wave number position in response to the application of stress or strain to a sample<sup>[17]</sup>. The method for obtaining well-defined Raman spectra of spider silk filaments was introduced by Gillespie et al.<sup>[18]</sup>. In addition, Lefèvre et al.<sup>[19-20]</sup> used Raman spectroscopy to analyze primary and secondary structures from the native liquid silk in the major ampullate gland to the fiber. Their examination demonstrated that Raman spectromicroscopy is particularly efficient for investigating all aspects of silk structure and production. Shao et al.<sup>[21]</sup> also employed Raman spectroscopy to demonstrate that differences in the mechanical properties were attributable to variations in the quantity of  $\beta$ -sheet contented in a silk fiber.

In this study, Raman spectroscopy was used to investigate structural changes, particularly with respect to  $\beta$ -sheet conformation, in spider dragline silk fibers obtained by different spinning methods: crawl spinning, drop spinning and artificial reeling at 20 mm/s.

## 2 Materials and methods

### 2.1 Spiders and silk fiber preparation

The spiders used in this study were *Nephila clavata*, from the campus of Shinshu University, Japan. Dragline silk samples were collected by the following methods:

(1)Crawl spinning: placed the spider on a black table, allowed it to walk for at least 60-80 cm, while

trailing silk behind it, silk was then collected.

(2)Drop spinning: placed the spider on a black table, collected the dragline silk when the spider vertically dropped off the edge.

(3)Artificial reeling: dragline silk was reeled directly from a restrained but fully awake spider at a drawing speed of 20 mm/s.

### 2.2 Methods

Raman spectroscopy measurements were performed with a HoloLab series 5000 Raman spectroscope (Kaiser optical systems, INC.). The 514 nm line of an Ar<sup>+</sup> laser was used. The laser beam was focused with a 50 $\times$  objective (Olympus BX51) to a diameter of 2  $\mu$ m, generating an intensity at the sample of 6 mW of power. The measurement time of a single spectrum was 110 s, and 10 measurements were obtained. Every sample was measured 3 times, and an average Raman spectrum was calculated.

### 2.3 Data analysis<sup>[20, 22]</sup>

All spectral manipulations were performed using Origin 7.5 (Origin Lab). The spectra were first corrected for a small fluorescence background over the 500-1 800 cm<sup>-1</sup> spectral range using a polynomial baseline. The data were 5-points smoothed, and a linear baseline was subtracted in the amide I region (1 750-1 570 cm<sup>-1</sup>).

Secondary structure composition was evaluated from the amide I band of the isotropic spectra. Because it consists of overlapping components due to the multiple secondary structures present in the sample, curve-fitting of the spectra have been necessary. The number and position of components of the experimental spectrum were determined using the following criteria in order of decreasing importance: (1)minimum number of components; (2) acknowledged secondary structures present in the considered system; (3) spectral criteria (shape of the experimental spectra, second derivatives and difference spectra.) and (4) generation of a reasonable fit (potentially requiring additional bands).

## 3 Results and discussion

### 3.1 Band assignments

The Raman spectrum of dragline silk fibers showed well-resolved peaks, including strong bands for the photosensitive aromatic amino acids tryptophan, tyrosine, and phenylalanine and for the amide I and amide III bands. The Raman spectrum in the region of 800 - 1 800 cm<sup>-1</sup> of dragline silk obtained by each spinning method is shown in Figure 1 and the Raman band assignments for silk listed in Table 1. The

Raman band exhibited a minor difference between silk fibers obtained by different spinning methods.

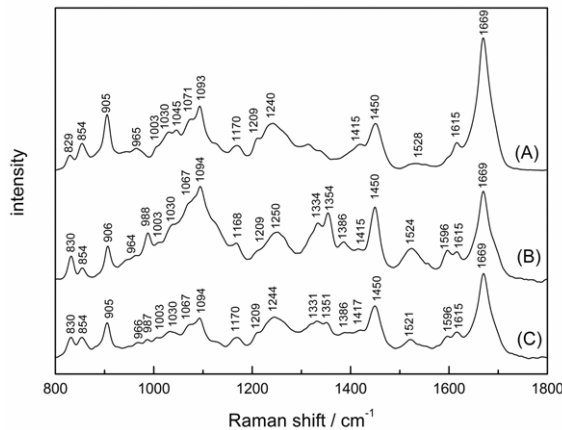


Figure 1 Raman spectra of *N. clavata* dragline silk fiber obtained by (A) artificial reeling at 20 mm/s, (B) crawl spinning, and (C) drop spinning

### 3.2 Comparison among spider dragline silk fiber obtained by different methods

Figure 1 shows the Raman spectra of dragline

silk fiber obtained by spider spinning (crawl and drop spinning), compare to that of silk fiber obtained by artificial reeling. In the drop spinning and artificial reeling spectra, both the amide I and amide III bands are centered at 1 669 and near 1 240  $\text{cm}^{-1}$ , respectively, showing that the proteins in the silk exist in a  $\beta$ -sheet conformation. For crawl-spun fibers, the amide III band shift to 1 250  $\text{cm}^{-1}$  is attributable to random coil. These data indicate an obvious conformational change from the random coil in crawl-spun to  $\beta$ -sheets in the drop- spinning and artificial-reeled fibers.

Other bands aside from the amide bands are changed when dragline silk fiber is obtained by different methods, particularly in the 1 300-1 400  $\text{cm}^{-1}$  region and near 988  $\text{cm}^{-1}$ . Two bands one approximately 988  $\text{cm}^{-1}$  and the other at 1 354  $\text{cm}^{-1}$  observed in the spectra of spider-spun silk, but these bands are absent in the spectrum of forcibly obtained silk. These bands mainly originate from the C-C skeletal stretch (988  $\text{cm}^{-1}$ ) and  $\text{CH}_2$  deformation (1 354  $\text{cm}^{-1}$ ).

Table 1 Position and assignment of different bands of *N. clavata* dragline silk fibers obtained by three spinning methods

Crawl spinning	Drop spinning	Artificial reeling at 20 mm/s	Assignment
830	830	829	Tyr
854	854	854	Tyr
906	905	905	Polyalanine
965	966	965	Ala
988	987		C-C stretch
1 003	1 003	1 003	Phe
1 030	1 031	1 030	Phe (in-plane stretching of benzene ring)
		1 045	Pro
1 067	1 067	1 075	Ser
1 094	1 094	1 093	$\text{C}\alpha$ - $\text{C}\beta$ stretching
1 126	1 126	1 126	Leu
1 168	1 170	1 170	Tyr
1 209	1 209	1 209	Tyr
1 252	1 244	1 240	Amide III (N-H bend +C-N stretching)
1 334	1 331		Ala
1 354	1 351		$\text{CH}_2$ deformation
1 386	1 386		C-C stretching of isoquinoline
1 415	1 417	1 415	Gly
1 450	1 450	1 450	$\text{CH}_2$ , $\text{CH}_3$ bending modes
1 524	1 521	1 528	C=C stretching of conjugated chain
1 596	1 596	1 596	Tyr
1 615	1 615	1 615	Tyr
1 669	1 669	1 669	Amide I (C=O stretching)

The doublet bands located near 830  $\text{cm}^{-1}$  and 854  $\text{cm}^{-1}$  can be useful for monitoring the microenvironment around tyrosyl residues<sup>[21, 23]</sup>. The tyrosyl doublet ratio (I854/I830) has been proposed as a mean of determining whether tyrosine residue is solvent when exposed or buried in a hydrophobic environment.

When the 850  $\text{cm}^{-1}$  band is more intense than the 830  $\text{cm}^{-1}$  band, the tyrosine residue is exposed. On the other hand, when I850 is less than I830, tyrosine residues are buried and tend to act as hydrogen donors. Figure 1 shows differences in the relative intensity of the tyrosine doublet at 830 and 854  $\text{cm}^{-1}$ . The 853  $\text{cm}^{-1}$

band for crawl- and drop-spun silks was less intense than the  $830\text{ cm}^{-1}$ , indicating that the tyrosyl residue was buried. The  $850\text{ cm}^{-1}$  band at for artificial reeled silk, however, was more intense than that at  $830\text{ cm}^{-1}$ , indicating that, for this fiber, the tyrosine residues are exposed. This result suggests that hydrogen bonds involving tyrosyl residues are stronger in the spider-spun silk than artificial-reeled silk.

### 3.3 Quantitative analysis of fibroin conformation

Typical curve-fitting results for dragline silk fibers created by different spinning methods are presented in Figure 2. An examination of these dragline silk fibers revealed that the presence of five amide I components, located typically near  $1\ 641$ ,  $1\ 655$ ,  $1\ 669$ ,  $1\ 684$  and  $1\ 700\text{ cm}^{-1}$ , and two bands at  $1\ 596$  and  $1\ 615\text{ cm}^{-1}$ , which are associated with tyrosine side-chain vibrations. Spectral decompositions are presented in Figure 2 for dragline silk fibers that were

obtained by all three spinning methods. The position, full width at half maximum, and the individual components resulting from this spectral decomposition are give in Table 2. From these decomposed spectra, the proportions of  $\alpha$ -helix,  $\beta$ -sheet, unordered and  $\beta$ -turn structures were calculated, and the obtained results are presented in Table 3. As observed in this table, silk fiber obtained by different spinning methods exhibits different secondary structure concentrations. Compared among three spinning method, the artificial reeled silk fibers have maximum  $\beta$ -sheet content value and minimum  $\alpha$ -helix content value is 42.94% and 8.48%, respectively. Crawl spun silk exhibited a maximum  $\alpha$ -helix content value and minimum  $\beta$ -sheet content value. These results mean that some of the  $\alpha$ -helix, and perhaps some other structures, are transformed into  $\beta$ -sheet structure during the spinning process.

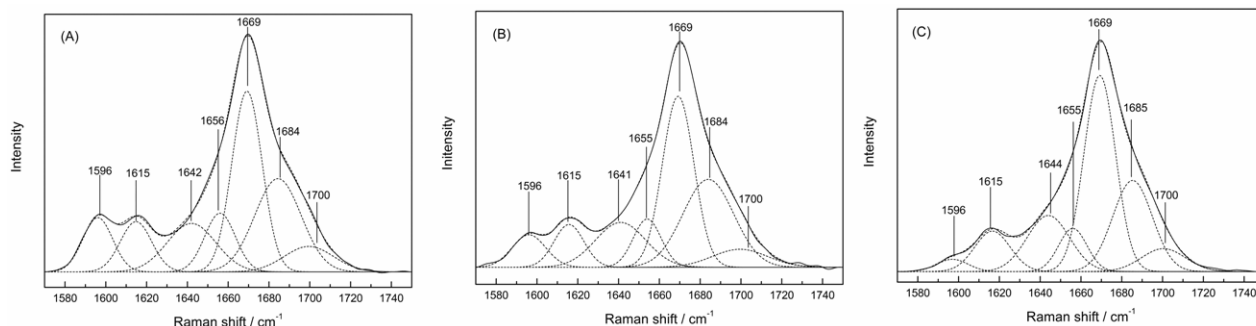


Figure 2 Band decomposition of the amide I region ( $1\ 570$ - $1\ 750\text{ cm}^{-1}$ ) of the polarized spectra for silks obtained by (A) crawl spinning, (B) drop spinning, and (C) artificial reeling at  $20\text{ mm/s}$

Table 2 Results of amide I curve-fitting of *N. clavata* dragline silk fibers obtained by three different spinning methods

		1	2	3	4	5	6	7
Assignment		Unordered		$\alpha$ -helix	$\beta$ -sheet	$\beta$ -turn	$\beta$ -turn	
Crawl spinning	Position / $\text{cm}^{-1}$	1 596	1 615	1 642	1 656	1 669	1 684	1 700
	FWHM / $\text{cm}^{-1}$	17	18	28	18	17	27	28
Drop spinning	Position / $\text{cm}^{-1}$	1 596	1 615	1 641	1 655	1 669	1 684	1 700
	FWHM / $\text{cm}^{-1}$	19	17	29	16	18	29	31
Artificial reeling at $20\text{ mm/s}$	Position / $\text{cm}^{-1}$	1 596	1 615	1 641	1 655	1 669	1 685	1 700
	FWHM / $\text{cm}^{-1}$	17	20	24	16	18	23	25

Table 3 Percentages of secondary structure of *N. clavata* dragline silk fibers obtained by three different spinning methods

	Unordered	$\alpha$ -helix	$\beta$ -sheet	$\beta$ -turn
Crawl spinning	15.51	11.79	35.97	36.71
Drop spinning	15.59	9.27	37.40	37.74
Artificial reeling at $20\text{ mm/s}$	16.59	8.48	42.94	31.99

These results indicate that the secondary structure of spider silk could be modified by altering the spider's spinning environment. Indeed, the differences in secondary structure can be used in interpretation of biomechanical data. Higher  $\beta$ -sheet content can improve the silk strength and stiffness<sup>[7]</sup>. These findings also

suggest the tenacity of spider dragline silk fiber obtained by artificial reeling at  $20\text{ mm/s}$  may be improved.

## 4 Conclusions

Raman spectroscopy is a useful tool for obtaining direct information on the secondary structural changes.

When a high-performance polymer fiber is deformed, the stress applied is transformed directly into structural deformation, this deformation of in both crystalline and amorphous regions of the fiber cause a change in bond lengths, bond angles and internal rotation angles, which lead to a shift in the Raman frequency for a particular vibrational mode.

In this work, the conformation of the proteins in *N. clavata* dragline silk fibers obtained by three spinning methods was characterized. The obtained silk fibers exhibited a common structure characterized by the presence of  $\beta$ -sheet, unordered,  $\beta$ -turn and  $\alpha$ -helix conformations. The presence of these secondary structures was determined through a curve-fitting procedure for the amide I band spectra, and the proportion of each within a fiber was found to vary with the spinning method. The quantity of  $\beta$ -sheet structures was greatly enhanced for silk fibers obtained by artificial reeling at 20 mm/s. This change may result in improved mechanical properties of dragline silk fiber, which has been helpful in designing an outstanding artificial spider silk.

## 5 Acknowledgements

This study was supported by a Grant-in-Aid for the Global COE program by the Ministry of Education, Culture, Sports, Science and Technology of Japan, as well as the Anhui International Science and Technology Cooperation Project, No. 12030603008. The authors express their thanks to Keiko Kakegawa for her technical support.

## References:

- [1] Hojo N. Structure of silk yarn part-B: Chemical structure and processing of silk yarn[M]. Trotman: Science Publishers, 2000: 175.
- [2] Yuksek M, Kocak D, Beyit A, et al. Effect of degumming performed with different type natural soaps and through ultrasonic method on the properties of silk fiber[J]. Advances in Environmental Biology, 2012, 6(2): 801-808.
- [3] Vollrath F and Knight D P. Liquid crystalline spinning of spider silk[J]. Nature, 2001, 410: 541-548.
- [4] Gosline J M, Guererre P A, Ortlepp C S et al. The mechanical design of spider: from fibroin sequence to mechanical function[J]. J Exp Biol, 1999, 202: 3295-3303.
- [5] Vollrath F. Strength and structure of spiders' silks[J]. Review in Molecular biotechnology, 2000, 74: 67-83.
- [6] Hayashi C Y, Shiply N H and Lewis R V. Hypotheses that correlate the sequence, structural, and mechanical properties of spider silk proteins[J]. Int J Biol Macromol. 1999, 24(2/3): 271-275.
- [7] Bratzel G and Buehler M J. Molecular mechanics of silk nanostructures under varied mechanical loading[J]. Biopolymers, 2011, 97(6): 408-416.
- [8] Boutry C and Blackledge T A. The common house spider alters the material and mechanical properties of orbweb silk in response to different prey[J]. Journal of Experimental Zoology. 2008, 309A(9): 542-552.
- [9] Dicko C, Vollrath F and Kenney J M. Spider silk protein refolding is controlled by changing pH[J]. Biomacromolecules, 2004, 5(3): 704-710.
- [10] Gaines W A, Sehorn M G and Marrcotte W R. Spidroin N-terminal domain promotes a pH-dependent association of silk proteins during self-assembly[J]. Journal of Biological Chemistry. 2010, 285: 40745-40753.
- [11] Eles P T and Michal C A. A DECODER NMR study of backbone orientation in *Nephila clavipes* dragline silk under varying strain and draw rate[J]. Biomacromolecules. 2004, 5(3): 661-665.
- [12] Vollrath F, Madsen B and Shao Z Z. The effect of spinning conditions on the mechanics of a spider's dragline silk[J]. Proc R Soc Lond Ser B-Biological Sciences, 2001, 268(1483): 2339-2346.
- [13] Vehoff T, Glišović A, Schollmeyer H, et al. Mechanical properties of spider dragline silk: humidity, hysteresis and relaxation[J]. Biophysical Journal. 2007, 93: 4425-4432.
- [14] Garrido M A, Elices M, Viney C, et al. Active control of spider silk strength: comparison of drag line spun on vertical and horizontal surfaces[J]. Polymer, 2002, 43: 1537-1540.
- [15] Herreo A M. Raman spectroscopy for monitoring protein structure in muscle food systems[J]. Critical Reviews in Food Science and Nutrition, 2008, 48(6): 512-513.
- [16] Rousseau M E, Lefèvre T, Beaulieu L, et al. Study of protein conformation and orientation in silkworm and spider silk fibers using Raman microspectroscopy[J]. Biomacromolecules, 2004,5(6): 2247-2257.
- [17] Sirichaisit J, Brookes V L, Young R J, et al. Analysis of structure/property relationships in silkworm (*Bombyx mori*) and spider dragline (*Nephila edulis*) silks using Raman spectroscopy[J]. Biomacromolecules. 2003, 4(2): 387-394.
- [18] Gillespie D B, Viney C and Yager P. Raman- Spectroscopic analysis of the secondary structure of spider silk fiber [M]//Kaplan D, Adams W W, Farmer B, et al. Silk polymers: materials science and biotechnology. Seattle: American Chemical Society, 1994: 155- 167.
- [19] Lefèvre T, Paquet-Mercier F, Rioux-Dubé J-F, et al. Structure of silk by Raman Spectromicroscopy: from the spinning glands to the fibers[J]. Biopolymers, 2011, 97(6): 322-336.
- [20] Lefèvre T, Rousseau M E and Pézolet M. Protein secondary structure and orientation in silk as revealed by Raman spectromicroscopy[J]. Biophysical Journal, 2007, 92: 2885-2895.
- [21] Shao Z, Vollrath F, Sirichaisitb J, et al. Analysis of spider silk in native and supercontracted states using Raman spectroscopy[J]. Polymer, 1999, 40: 2493-2500.
- [22] Rousseau M E, Beaulieu L, Lefèvre T, et al. Characterization by Raman microspectroscopy of the strain-induced conformational transition in fibroin fibers from the silkworm *Samia cynthia ricini*[J]. Biomacromolecules, 2006, 7(9): 2512-2521.
- [23] Maiti N C, Apetri M M, Zagorski M G, et al. Raman spectroscopic characterization of secondary structure in natively unfolded proteins: alpha-synuclein[J]. Journal of the American Chemical Society, 2004, 126(8): 2399-2408.